

AN INTEGRATED OPTIMIZATION AND SURROGATE ANALYSIS OF LARGE AIRCRAFT IN CONCEPTUAL DESIGN

Xiaozhe Wang¹, Zhiqiang Wan¹, and Chao Yang¹

¹ School of Aeronautic Science and Engineering
Key Laboratory of Aircraft Advanced Design Technology, Ministry of Industry and Information
Beihang University, Beijing, China, 100191
wangxiaozhemvp@buaa.edu.cn

Keywords: Large aircraft, Integrated optimization design, Aeroelasticity, Conceptual phase, Kriging

Abstract: The multidisciplinary design optimization (MDO) has the potential in large aircraft design. An integrated optimization method of large aircraft in conceptual phase is presented. The objective is the minimum stiffness of a beam-frame wing structure subject to aeroelastic, aerodynamic and stability constraints. The aeroelastic responses are calculated by commercial software MSC. Nastran, and the cruise stability is evaluated by the linear small-disturbance equations. A viscous-inviscid iteration method provided by commercial CFD solver MGAERO is used for computing the flow over the model. To reduce the computational burden and explore the entire design space, the evaluation of the responses in optimization is performed using Kriging model. The optimization method is validated by application to the wing of a complete aircraft. All the responses are computed in the trim condition with a fixed maximum takeoff weight. Genetic algorithm (GA) is utilized for global optimizations, and the optimal jig shape, the elastic axis positions and the stiffness distribution of the wing can be attained simultaneously, avoiding the iteration design.

1 INTRODUCTION

In conventional design methods of the large aircraft, the optimizations of aerodynamics, structure and stability are performed in a specific sequence. The aerodynamic shape under typical cruise conditions is achieved firstly, which has benefit a great deal from the utilization of optimization tools and high fidelity computational fluid dynamics (CFD) tools based on the Reynolds-averaged Navier–Stokes (RANS) equations [1,2]. The maximum lift-to-drag ratio is often regarded as the objective subject to reasonable geometric shape and pressure distribution, applying parameterization methods suitable for airfoils [3], the wing planform [4-6] or adaptive wing shapes [1]. Many engineering optimization problems have been well solved.

The structure design follows referring to the certain aerodynamic shape. The structure design of a large aircraft wing routinely contains stiffness design [7], structural layout design [8], structural size design [9] and structure design with different kinds of uncertainties [10,11]. The structural property parameterization (skin/web thickness, flange area, ply orientation, etc.) are much more convenient in finite element analysis (FEA), and the objective is often the structural mass subject to multiple constraints (deformation, stability, flutter, stress/strain, failure, etc.). Aeroelastic tailoring is a typical optimization, which is applied widely in

engineering [12]. The jig shape can also be attained with the predefined aerodynamic shape and structure [13].

Nevertheless, as a sequential design, the conventional method depends on engineering experience excessively. The significant limitation may cause iteration design, resulting in inefficiency. The multidisciplinary design optimization (MDO) could take disciplines containing aerodynamics, structure, aircraft flight dynamics, etc. into consideration simultaneously, which can solve the limitations and has been applied in the modern aircraft design [14,15]. The MDO should be employed in conceptual phase of large aircraft design. A crucial challenge of MDO is its massive computation burden, especially for CFD simulations based on RANS equations. Though RANS method can simulate intricate turbulence and shedding vortex, some inviscid/viscous iteration methods are more suitable for the large aircraft design in cruise conditions with moderate flow separation [16-18].

To reduce the computational burden and help to a great extent in better exploration and exploitation of the design space, surrogate-based optimization (SBO) has recently found widespread use owing to its promising potential [19-21]. As a response surface model (RSM), Kriging model is developed in the field of spatial statistics and geostatistics compared with the polynomial-based model, which is the most widely used RSM [22, 23].

A gradient-based algorithm has the advantage of rapidity, but it is apt to converge to a local optimum solution, and the derivatives are also difficult to calculate [24]. The evolutionary algorithms are suitable for these MDO problems, and Genetic algorithm (GA) is used most widely as a global algorithm [25]. GA needs to calculate a large number of individuals to search a global optimum, but the computation burden of FEA or CFD is unacceptable. Therefore, the combination of GA and surrogate models is an efficient approach.

In this paper, an integrated optimization method of the large aircraft design in conceptual phase is proposed, considering the disciplines of aerodynamics, structure and stability. The analysis model is a complete aircraft configuration. The doublet-lattice method and FEA are used for static aeroelastic and flutter analysis. The lift-to-drag ratio is evaluated by an inviscid/viscous iteration method composed of a CFD tool solving the Euler equations and a viscous correction method. The linear small-disturbance method is used for the evaluation of stability of aircraft flight dynamics. Kriging method is adopted for surrogate analysis to search the optimum solution effectively, and Latin hypercube sampling is utilized in the design of experiment (DoE). GA is utilized for the global optimization. The objective is to seek the minimum stiffness of a beam-frame structure wing subject to the aeroelastic constraints, the stability constraint and the aerodynamic constraint in a trim condition. The optimal jig shape, the elastic axis positions and the stiffness distribution of the wing can be attained simultaneously.

2 METHODOLOGY

2.1 Aerodynamics Analysis

The commercial code MGAERO is employed as a CFD solver to evaluate the lift-to-drag ratio. It uses a multigrid calculation procedure with an equally spatial Cartesian mesh to discretize the governing Euler equations for inviscid compressible flow. The shock wave drag and the induced drag can also be decomposed from the total inviscid drag via the far field drag analysis [27].

The solver employs Cartesian blocks of meshes which do not require grids aligned to the body surface, which greatly eases the grid generation. The spatial mesh deformation can be implemented effortlessly by moving the finest level mesh according to the shape and the maximum deflection of the wing [13,18]. For this reason, the solver is ideally suited for the integrated optimization.

The viscous correction is accomplished via the transpiration technique. The surface boundary condition is modified based upon the transpiration velocity, which is a function of the boundary layer edge velocity, the displacement thickness and the local density. The boundary layer characteristics are computed along surface streamlines [18]. The boundary layer correction is an iterative process that may require 3 to 5 viscous/inviscid cycles to complete [26].

2.2 Aeroelasticity Analysis

The commercial code MSC. Nastran is employed for the analysis of static aeroelasticity and flutter. The basic equation of static aeroelasticity is [10]:

$$(\mathbf{K}_{aa} - \bar{q}\mathbf{Q}_{aa})\mathbf{u}_a + \mathbf{M}_{aa}\ddot{\mathbf{u}}_a = \bar{q}\mathbf{Q}_{ax}\mathbf{u}_x + \mathbf{P}_a \quad (1)$$

where the subscript a means the structural displacement vector set of analysis freedom, \mathbf{K}_{aa} is the structural stiffness matrix, \mathbf{Q}_{aa} is the matrix of aerodynamic influence coefficients, \mathbf{M}_{aa} is the structural mass matrix, \mathbf{Q}_{ax} is the matrix of unit aerodynamic loads, \mathbf{u}_a is the structural deformation vector, $\ddot{\mathbf{u}}_a$ is the acceleration vector of rigid body motion, \mathbf{u}_x is the vector of aerodynamic trim parameters (e.g., angle of attack, elevator deflection), which is used to define the deflection of the aerodynamic control surface and the overall rigid motion of the aircraft, \mathbf{P}_a is the vector of applied loads, and \bar{q} is the dynamic pressure.

The equation of the p - k flutter analysis method is [12]:

$$\left[\left(\frac{V}{b} \right)^2 p^2 \mathbf{M} + \frac{V}{b} p \mathbf{B} + \mathbf{K} - \frac{1}{2} \rho V^2 \left(\mathbf{Q}^R + \frac{p}{k} \mathbf{Q}^I \right) \right] \mathbf{u} = 0 \quad (2)$$

where \mathbf{M} is the generalized mass matrix, \mathbf{B} is the generalized damping matrix, \mathbf{K} is the generalized stiffness matrix, V is the flow speed, b is the reference chord length, p is the eigenvalue, ρ is the air density, k is the reduced frequency, \mathbf{u} is the vector of the generalized structural degree of freedom, and the superscripts R and I represent the real and imaginary parts, respectively. The surface spline method [28] is utilized for the displacement interpolation between the structural grid points and the aerodynamic surface grid points.

2.3 Stability Analysis

The stability of aircraft flight dynamics is evaluated via the linear small-disturbance theory, so the aircraft flight dynamics equations can be decoupled. The longitudinal stability and lateral stability can be considered separately, and the normal state-space equation of longitudinal/lateral stability in the cruise condition is [29]:

$$\dot{\mathbf{x}} = \mathbf{A}\mathbf{x} + \mathbf{B}\mathbf{u} \quad (3)$$

where \mathbf{A} is the system matrix, \mathbf{B} is the control matrix, \mathbf{x} is the state vector, and \mathbf{u} is the control vector. \mathbf{A} and \mathbf{B} are constructed by the aerodynamic derivatives, the mass property

and the aerodynamic coefficients, and \mathbf{x} is composed by the disturbed flight parameters, and \mathbf{u} is composed by the deflections of control surfaces.

The control surface efficiency considering the elastic deformation effect is expressed as [9]:

$$\eta = (\partial C_m / \partial \delta)_e / (\partial C_m / \partial \delta)_r \quad (4)$$

where C_m is the moment coefficient, and δ is the control surface deflection. The subscript e denotes the elastic value, and the subscript r denotes the rigid value.

2.4 Kriging Method

The Kriging model used here expresses the unknown function $y(\mathbf{x})$ as [22,23]:

$$y(\mathbf{x}) = f(\mathbf{x}) + z(\mathbf{x}) \quad (5)$$

where \mathbf{x} is an m -dimensional vector (m design variables), $f(\mathbf{x})$ is a constant global model, and $z(\mathbf{x})$ represents a local deviation from the global model. The constant global model uses a polynomial regression (not greater than second order) to construct the response surface. The local deviation at an unknown point \mathbf{x} is expressed using stochastic processes. Sample points are interpolated with the correlation function to estimate the trend in the stochastic processes.

The correlation between $z(\mathbf{x}^i)$ and $z(\mathbf{x}^j)$ is strongly related to the distance between the two corresponding \mathbf{x}^i and \mathbf{x}^j , and the distance is expressed as:

$$d(\mathbf{x}^i, \mathbf{x}^j) = \sum_{k=1}^m \theta_k |x_k^i - x_k^j|^2 \quad (6)$$

where θ_k is the correlation parameter. The method weighs all design variables equally, and the Gaussian random function used as the correlation function is defined as follows:

$$Corr[z(\mathbf{x}^i), z(\mathbf{x}^j)] = \exp[-d(\mathbf{x}^i, \mathbf{x}^j)] \quad (7)$$

In order to improve the accuracy of Kriging model, θ_k is adjusted to minimized the predictive error via an optimization method.

2.5 Optimization Algorithm

The integrated optimization is a typical optimization problem involving the search of design variables (DVs) in the n_{dv} -dimensional space to minimize the objective function while satisfying the n_{con} constraints [12,23]:

$$\begin{aligned} \text{Min.} \quad & \mathbf{F}(\mathbf{v}) \\ \text{S.T.} \quad & g_j(\mathbf{v}) \leq 0 \quad j = 1, 2, \dots, n_{con} \\ & v_i^{lower} \leq v_i \leq v_i^{upper} \quad i = 1, 2, \dots, n_{dv} \end{aligned} \quad (8)$$

where $F(\mathbf{v})$ is the objective function, $g_j(\mathbf{v})$ are the constraints, and v_i^{lower} and v_i^{upper} are the lower and upper bounds of the DVs, respectively.

GA has a good search in the global design space, and it is utilized for the integrated optimization.

3 OPTIMIZATION STRATEGY

3.1 Baseline Model

The baseline CFD aerodynamic models are separated into the jig shape and the cruise shape. The cruise shape is transformed from the jig shape and the structural deformation, and the aerodynamic responses of cruise shape are calculated. Because the wingtip displacement is much less than the spanwise length, it is assumed that only the structural deformation about z axis is considered to construct the cruise shape [13]. The surface and space discretization of the CFD model is shown in Figure 1.

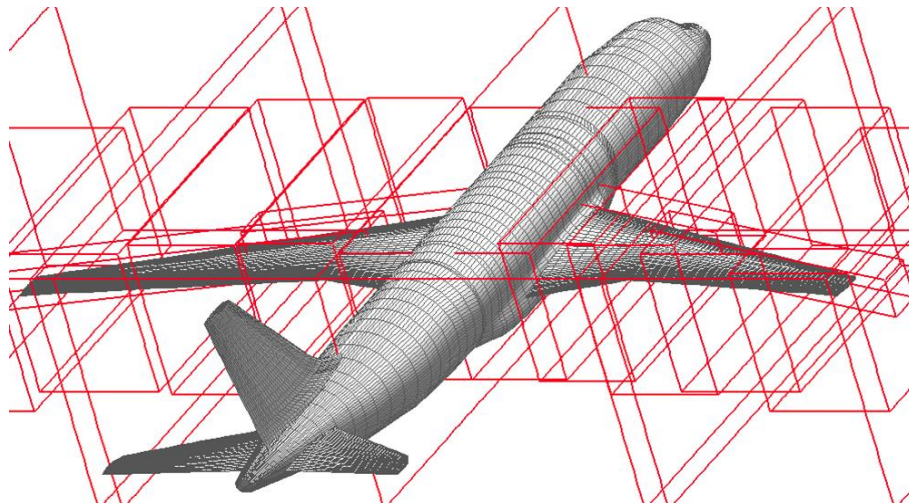


Figure 1: Surface and space discretization of CFD model

The space of a symmetric half model is discretized into 7 levels with 1637429 grids. The baseline aeroelastic models are shown in Figure 2.

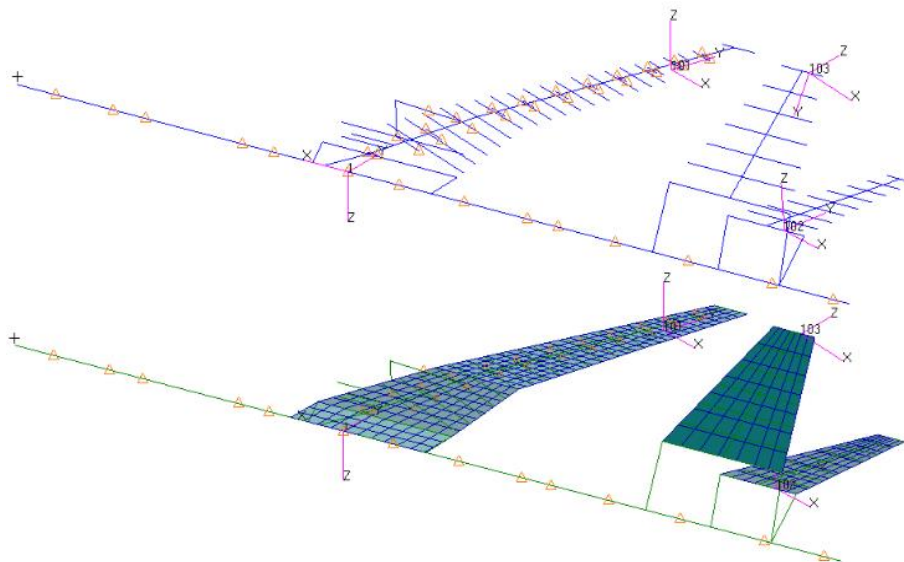


Figure 2: Baseline aeroelastic models: (a) Structural model and (b) aerodynamic model

Within this beam-frame finite element model, the wing stiffness characteristics are simulated by a variable cross-section beam from the root to the tip, and the mass characteristics are simulated by concentrated mass. Aluminium is applied as the material for the main beam of the wing. The body, tail and fin are simulated with rigid elements. The wing aerodynamic

surface is divided into 6 groups and 282 elements, with the airfoil camber considered in calculation.

The geometry shape of a high-aspect-ratio backswept wing can be parameterized with 7 parameters, including the inboard/outboard taper ratio, the inboard/outboard aspect ratio, the sweep angel of the leading edge (5 planform parameters), the inner/outer dihedral angle, and the wing root length remains constant. For a beam-frame structure model, 3 other parameters are used to parameterize the elastic axis positions at the root, the kink and the tip, respectively.

3.2 Objective Function and Constraints

In the conceptual phase of the large aircraft design, the stiffness distribution along the spanwise direction of the wing can be expressed as an exponential function with 9 variables [7]:

$$\begin{aligned} EI_{xx}(y) &= a_1 \cdot e^{b_1 \cdot y} + c_1 \\ EI_{yy}(y) &= a_2 \cdot e^{b_2 \cdot y} + c_2 \\ GJ(y) &= a_3 \cdot e^{b_3 \cdot y} + c_3 \end{aligned} \quad (9)$$

where a_i, b_i, c_i are the stiffness DVs, and y is the spanwise position. The stiffness of the cross section can be expressed as EI_{xx}, EI_{yy}, GJ , and the mass can be expressed as ρS . For the constant E, J and ρ , the stiffness is equivalent to the mass [30]:

$$(EI_{xx} + EI_{yy} + GJ)l \propto \rho S l \quad (10)$$

where l is the reference length of the wing. Therefore, the objective is to minimize $\sum(EI_{xx} + EI_{yy} + GJ) \times l$.

The specific constraints are as follows:

- (1) the maximum displacement of z direction at the wing tip is less than 7% of the semi-span;
- (2) the maximum torsion at the wing tip is less than 2.14° ;
- (3) the flutter speed at sea level is greater than 320 m/s;
- (4) the total drag is less than the baseline drag;
- (5) the aileron efficiency is greater than 60%;

In the cruise flight condition, the wing deformation of the large aircraft is within the linear theory of elasticity, so the displacement is required to be less than 7% of the semi-span. The elastic deformation may reduce the local angle of attack (AOA), so the maximum torsion at the wing tip should also be constrained.

3.3 Flowchart

The optimization flowchart is shown in Figure 3.

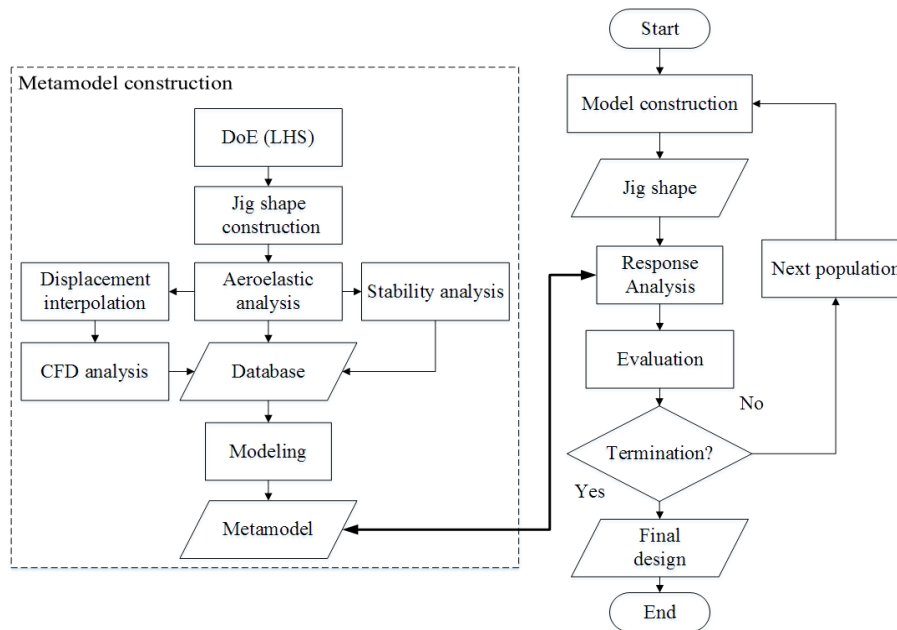


Figure 3: Optimization flowchart

First, the Kriging model is constructed. In order to extract as much information as possible from a limited set of computer experiments on the whole design space, 1997 samples representing all portions of the design space are selected with the help of LHS as DoE. Then, the aerodynamic response, the aeroelastic response and the stability response are evaluated via parallel computing, and the normalized value is chosen as the database to construct Kriging model. Besides, another 100 samples are also selected by LHS to validate the prediction accuracy of Kriging model.

4 RESULT ANALYSIS

4.1 Accuracy Analysis

The accuracy of Kriging model is verified, and the relative errors are shown in Figure 4.

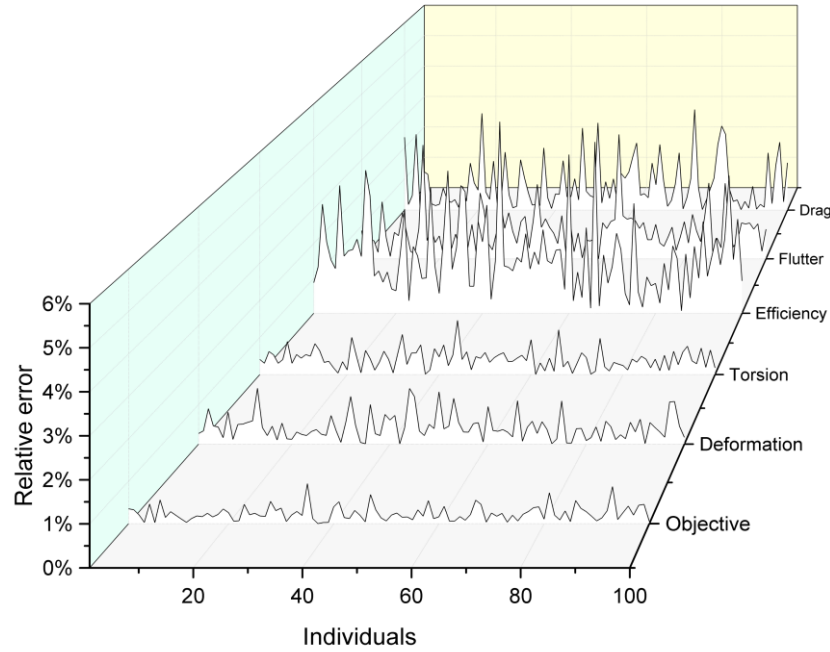


Figure 4: Accuracy of Kriging model

The relative errors of objective (stiffness), deformation (wingtip displacement), torsion (wingtip torsion), efficiency (aileron efficiency), flutter (whether the flutter speed is less than 320 m/s) and drag (the total drag) all satisfy the engineering requirement. Kriging model has adequate accuracy, and it can be used for the response prediction instead of FEA.

4.2 Response Analysis

The response comparison is shown in Table 1.

Response	Baseline	FEA	Kriging	Validation	Constraint
Objective	327	342	250	253	—
Wingtip deformation	5.34%	6.07%	4.8%	5.1%	<7%
Wingtip torsion	2.04°	2.05°	1.7°	1.8°	<4.5°
Total drag	64863N	64661N	64358N	64788N	<64863N
Flutter speed	450m/s	342m/s	450m/s	450m/s	>320m/s
Aileron efficiency	64.3%	65.5%	71.1%	69.4%	>60%

Table 1: Response comparison

The predictions and validations of the optimum using Kriging method satisfy all the given constraints. The surrogate analysis helps to a great extent in the better exploration of the design space, and all the performances are improved.

The comparison of cruise shapes is shown in Figure 5.

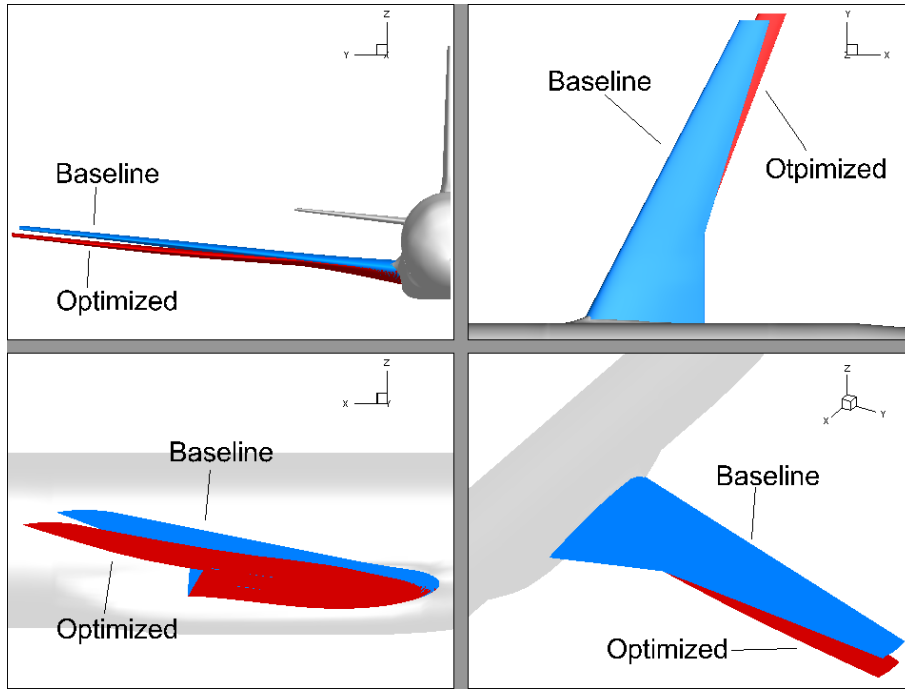


Figure 5: Comparison of the cruise shapes

At the flight condition of 0.785 Mach, the local shock drag appears, so the optimal cruise shape with a larger sweep angle has less drag. The supersonic region area of the optimal wing is less than the baseline one.

As the optimization objective, the comparison of stiffness distribution is shown in Figure 6.

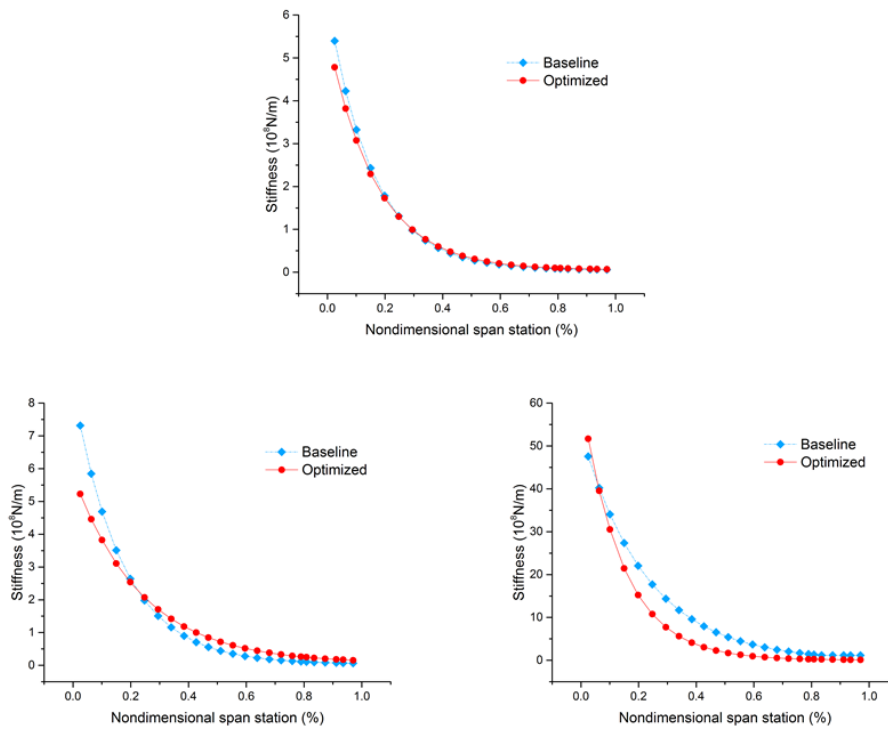


Figure 6: Stiffness curves along the spanwise direction (torsional, vertical bending, and horizontal bending)

The vertical bending stiffness decreases, especially at the region near the root, while the horizontal bending and torsional stiffness increase. The stiffness distribution near the wingtip of these two models is similar.

Figure 7 shows the comparisons of the surface pressure distribution and the airfoil pressure distribution of different positions.

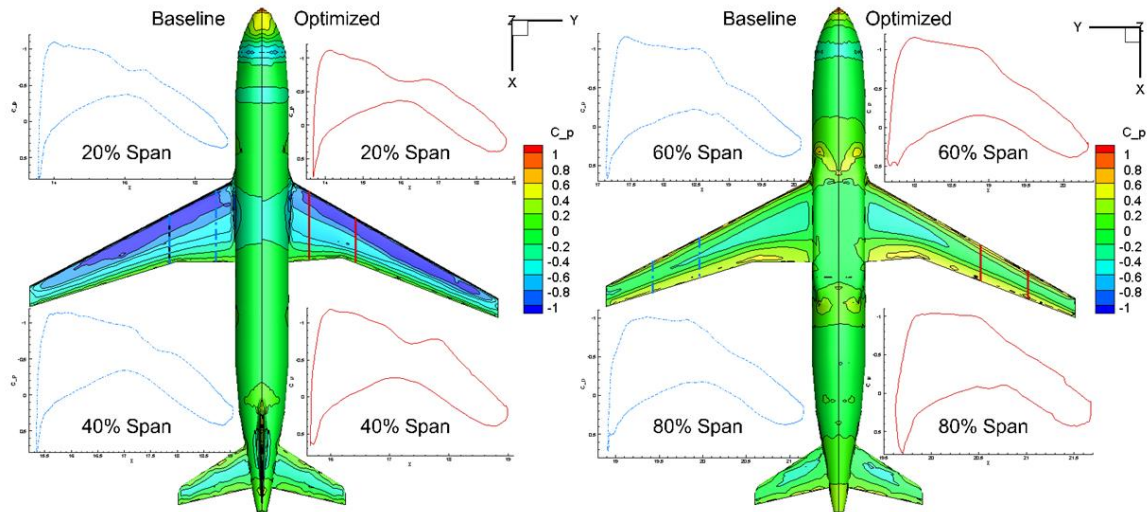


Figure 7: Comparison of surface pressure (upper and lower surfaces)

Since the change of the aerodynamic shape of the wing and the fixed takeoff weight, both the upper and lower surface pressure distribution varies. The pressure of the region near the wing changes a lot, while the other regions remain constant.

4.3 Stability Analysis

Figure 8 shows the comparison of the stabilities of the large aircraft.

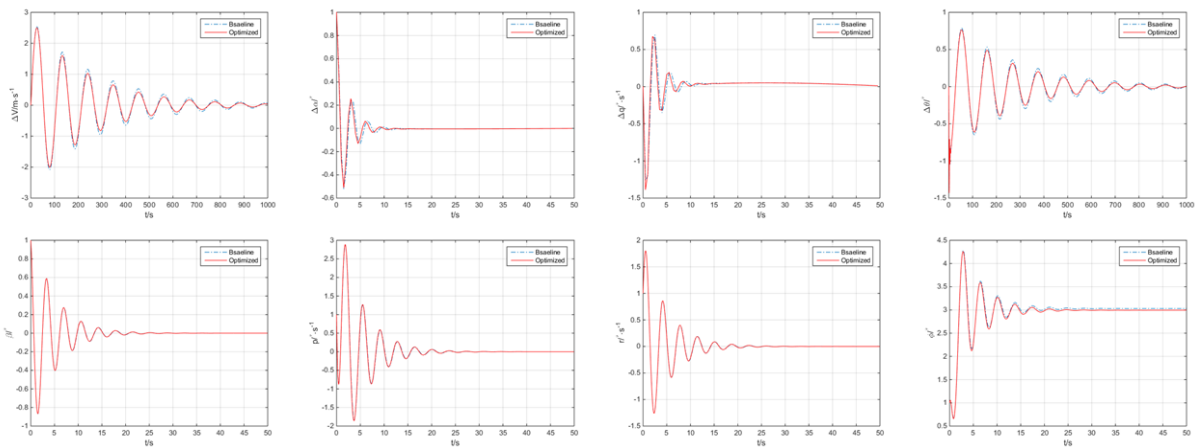


Figure 8: Comparison of stability

The perturbation responses of velocity, AOA, pitch rate, pitch angle, side angle, roll rate, yaw rate and roll angle all converge to zero. The optimized result has both longitudinal stability and lateral stability.

5 CONCLUSION

An integrated optimization method of the large aircraft design in conceptual phase is proposed. Kriging method is utilized for better exploration and exploitation of the design space, and GA ensures the global optimization. The method considers the complex coupling effect and examines the tradeoff of aerodynamics, structure and stability. The optimal jig shape, the elastic axis positions and the stiffness distribution of the wing can be attained simultaneously, and the iteration design can be avoided.

The results indicate that the weight can be reduced much satisfying all the specific constraints. The potential in exploring the entire design space with a good time saving confirms the utility of surrogate models in the conceptual design phases because it helps and guides to attain the potentially optimal design cases without recourse to huge computations. The conceptual design results of both aerodynamics and structure are important references for the preliminary design and the further complete design.

6 REFERENCES

- [1] Lyu, Z. and Martins, J. R. R. A. (2015). Aerodynamic Shape Optimization of an Adaptive Morphing Trailing-Edge Wing. *Journal of Aircraft*, 52(6), 1951-1970.
- [2] Chen, S., Lyu, Z., Kenway, G. K. W. and Martins, J. R. R. A. (2016). Aerodynamic Shape Optimization of Common Research Model Wing–Body–Tail Configuration. *Journal of Aircraft*, 53(1), 276-293.
- [3] Zhang, Y. F., Fang, X. M., Chen, H. X., Fu, S., Duan, Z. Y. and Zhang, Y. J. (2015). Supercritical natural laminar flow airfoil optimization for regional aircraft wing design. *Aerospace Science and Technology*, 43, 152-164.
- [4] Morris, A. M., Allen, C. B. and Rendall, T. C. S. (2014). Aerodynamic shape optimization of a modern transport wing using only planform variations. *Proceedings of the Institution of Mechanical Engineers, Part G: Journal of Aerospace Engineering*, 223(G6), 843-851
- [5] Zhao, T., Zhang, Y. F., Chen, H. X., Chen, Y. C. and Zhang, M. (2016). Supercritical wing design based on airfoil optimization and 2.75D transformation. *Aerospace Science and Technology*, 56, 168-182.
- [6] Kenway, G. K. W. and Martins, J. R. R. A. (2016). Multipoint Aerodynamic Shape Optimization Investigations of the Common Research Model Wing. *AIAA Journal*, 54(1), 113-128.
- [7] Liu, D. Y., Wan, Z. Q., Yang, C. and Yang, T. Primary Modeling and Analysis of Wing Based on Aeroelastic Optimization. In: 51st AIAA/ASME/ASCE/AHS/ASC Structures, Structural Dynamics, and Materials Conference
 18th, Orlando, Florida, 12-15 April 2010, AIAA 2010-2719.
- [8] Wan, Z. Q., Liu, D. Y., Tang, C. H. and Yang, C. (2012). Studies on the influence of spar position on aeroelastic optimization of a large aircraft wing. *Science China-Technological Sciences*, 55(1), 117-124.
- [9] Liang, L., Wan, Z. Q. and Yang, C. (2012). Aeroelastic optimization on composite skins of large aircraft wings. *Science China-Technological Sciences*, 55(4), 1078-1085.
- [10] Wan, Z. Q., Xiao, Z. P. and Yang, C. (2011). Robust Design Optimization of Flexible Backswept Wings with Structural Uncertainties. *Journal of Aircraft*, 48(5), 1806-1809.

- [11] Wan, Z. Q., Zhang, B. C., Du, Z. L. and Yang, C. (2014). Aeroelastic two-level optimization for preliminary design of wing structures considering robust constraints. *Chinese Journal of Aeronautics*, 27(2), 259-265.
- [12] Wan, Z. Q., Yang, C. and Zou, C. Q. Design Studies of Aeroelastic Tailoring of Forward-Swept Composite Aircraft Using Hybrid Genetic Algorithm. In: 44th AIAA/ASME/ASCE/AHS Structures, Structural Dynamics, and Materials Conference, Norfolk, Virginia, 7-10 April 2003, AIAA 2003-1491.
- [13] Wan, Z. Q., Liang, L. and Yang, C. (2014). Method of the Jig Shape Design for a Flexible Wing. *Journal of Aircraft*, 51(1), 327-330.
- [14] Yang, G. W., Chen, D. W. and Cui, K. (2009). Response Surface Technique for Static Aeroelastic Optimization on a High-Aspect-Ratio Wing. *Journal of Aircraft*, 46(4), 1444-1450.
- [15] Zhang, K. S., Han, Z. H., Li, W. J. and Song, W. P. (2008). Coupled Aerodynamic/Structural Optimization of a Subsonic Transport Wing Using a Surrogate Model. *Journal of Aircraft*, 45(6), 2167-2170.
- [16] Zhu, Z. Q. and Ma, X. (1991). An inverse integral 3D compressible boundary layer method and coupling with transonic inviscid solution. *Acta Mechanica*, 89(1), 187-208.
- [17] Sekar, W. K. and Laschka, B. (2005). Calculation of the transonic dip of airfoils using viscous-inviscid aerodynamic interaction method. *Aerospace Science and Technology*, 9(8), 661-671.
- [18] Zhang, M. L., Yang, C. and Wan, Z. Q. Aerodynamic shape optimization and static aeroelastic analysis of a morphing trailing edge wing. In: AIAA SciTech, 54th AIAA Aerospace Sciences Meeting, San Diego, California, USA, 4-8 January 2016, AIAA 2016-1783.
- [19] Song, W. B. and Keane, A. J. (2007). Surrogate-based aerodynamic shape optimization of a civil aircraft engine nacelle. *AIAA Journal*, 45(10), 2565-2574.
- [20] Boulkeraa, T., Ghenaiet, A., Mendez, S. and Mohammadi, B. (2014). A numerical optimization chain combining computational fluid dynamics and surrogate analysis for the aerodynamic design of airfoils. *Proceedings of the Institution of Mechanical Engineers, Part G: Journal of Aerospace Engineering*, 228(11), 1964-1981.
- [21] Allen, C. B. and Rendall, T. C. S. (2013). CFD-based optimization of hovering rotors using radial basis functions for shape parameterization and mesh deformation. *Optimization Engineering*, 14(1), 97-118.
- [22] Jeong, S., Obayashi, S. and Yamamoto, K. (2006). A Kriging-based probabilistic optimization method with an adaptive search region. *Engineering Optimization*, 38(5), 541-555.
- [23] Wan, Z. Q., Wang, X. Z. and Yang, C. (2016). A Highly Efficient Aeroelastic Optimization Method Based on a Surrogate Model. *International Journal of Aeronautical and Space Sciences*, 17(4), 491-500.
- [24] Li, C. M. (2009). *Optimization method*. Nanjing, China: Southeast University Press, (in Chinese).
- [25] Manan, A., Vio, G. A., Harmin, M. Y. and Cooper, J. E. (2010). Optimization of aeroelastic composite structures using evolutionary algorithms. *Engineering Optimization*, 42(2), 171-184.
- [26] Analytical methods, INC. (2010). *MGAERO User's Manual Version 3.5*. Redmond, Washington, USA.

- [27] Dam, van C. P., Nikfetrat, K., Wong, K. and Vijgen, P. M. H. W. (1995). Drag prediction at subsonic and transonic speeds using Euler methods. *Journal of Aircraft*, 32(4), 839-845.
- [28] Harder, R. L. and Desmarais, R. N. (1972). Interpolation Using Surface Splines. *Journal of Aircraft*, 9(2), 189–191.
- [29] Fang, Z. P., Chen, W. C. and Zhang, S. G. (2005). *Flight Dynamics of Aircraft*. Beijing, China: Beihang University Press, (in Chinese).
- [30] Gong Y N. (2001). *Structural Mechanics*. Beijing, China: Beihang University Press, (in Chinese).

ACKNOWLEDGMENTS

This work was supported by the National Key Research and Development Program (2016YFB0200703).

COPYRIGHT STATEMENT

The authors confirm that they, and/or their company or organization, hold copyright on all of the original material included in this paper. The authors also confirm that they have obtained permission, from the copyright holder of any third party material included in this paper, to publish it as part of their paper. The authors confirm that they give permission, or have obtained permission from the copyright holder of this paper, for the publication and distribution of this paper as part of the IFASD-2017 proceedings or as individual off-prints from the proceedings.